Alexandria Engineering Journal (2023) 64, 141–154

HOSTED BY

Alexandria University

Alexandria Engineering Journal

www.elsevier.com/locate/aej
www.sciencedirect.com

Analytical solution of stability and vibration problem of clamped cylindrical shells containing functionally graded layers within shear deformation theory

A.H. Sofiyev [a,b,c,*], N. Fantuzzi [d]

[a] Department of Civil Engineering, Engineering Faculty, Suleyman Demirel University, 32260 Isparta, Turkey
[b] Information Technology Research and Application Center Member of Consultancy Board of ITRAC Center, Istanbul Commerce University, Beyoglu 34445, Istanbul, Turkey
[c] Scientific Research Centers for Composition Materials of UNEC-Azerbaijan State Economics University, 1001/Baku, Azerbaijan
[d] Department of Civil, Chemical, Environmental, and Materials Engineering, University Bologna, Italy

Received 1 July 2022; revised 23 July 2022; accepted 16 August 2022
Available online 06 September 2022

KEYWORDS

FGM coatings;
Vibration;
Stability;
Sandwich cylindrical shells;
Clamped edges;
Critical parametrs;
Transverse shear stress functions

Abstract The aim of the study is to present a new approach to the analytical solution of the vibration and stability problem of clamped sandwich cylindrical shells (SCSs) covered by functionally graded (FG) coatings under an axial compressive load in the framework of shear deformation theory (ST). After modeling the micro and macro mechanical properties of FG coated SCSs with various configurations, the constitutive relations and basic equations are derived depending on the stress, deflection and two angles of rotation functions using modified Donnell type theory. An attempt is made to analytically solve the fundamental differential equations for SCSs covered by FG coatings using novel approximation functions satisfying the clamped boundary conditions. Three different shear stress functions (SSFs) such as parabolic shear stress function (Par-SSF), cosine-hyperbolic shear stress function (Cos-Hyp-SSF) and uniform shear stress function (U-SSF) are used in the analysis. After confirming the accuracy of the obtained results, the influences of coating profiles, volume fractions and layer arrangement variations on the critical parameters for three different transverse shear stress functions are investigated in detail.

© 2022 THE AUTHORS. Published by Elsevier BV on behalf of Faculty of Engineering, Alexandria University. This is an open access article under the CC BY-NC-ND license (http://creativecommons.org/licenses/by-nc-nd/4.0/).

1. Introduction

Since sandwich structures are increasingly being used in spacecraft, nuclear reactors, shipping, automotive and other technical applications due to their lightness and high structural

* Corresponding author at: Department of Civil Engineering, Engineering Faculty, Suleyman Demirel University, 32260 Isparta, Turkey.
E-mail addresses: abdullahavey@sdu.edu.tr (A.H. Sofiyev), nicholas.fantuzzi@unibo.it (N. Fantuzzi).

Peer review under responsibility of Faculty of Engineering, Alexandria University.

https://doi.org/10.1016/j.aej.2022.08.024
1110-0168 © 2022 THE AUTHORS. Published by Elsevier BV on behalf of Faculty of Engineering, Alexandria University.
This is an open access article under the CC BY-NC-ND license (http://creativecommons.org/licenses/by-nc-nd/4.0/).

performance, many fundamental studies of their behavior have been carried out in the literature [1–3]. In modern technology, coatings made of traditional and new generation composites are frequently used to increase the service life and performance of structural elements. One of the best coating types that regulate the stress distribution is FGMs in today's technological conditions. Today's technology can give a predetermined material appearance to coatings made of FGMs, in other words, the thermomechanical properties of such coatings can be changed continuously in the direction of thickness. Therefore, the thermo-mechanical properties of the FGMs constituting the coatings are a function of the thickness coordinate and are almost equal to the material properties of the layer at the bottom or the top of the coating, as well as changing as a continuous function towards the top or bottom of the coating. This superior feature of FGMs can prevent incompatibilities between the top or bottom layer of the structural member and the FGM coating. Since FGMs, produced by a group of Japanese scientists within the framework of a national project, were originally intended to be used as thermal barriers in spacecraft, their use as coatings on structural elements has been more common compared to other applications [4,5].

After these studies, serious scientific studies that shed light on the construction, production techniques, mechanical and thermal properties of coatings made of FGMs have been carried out and their superior properties compared to traditional composites have been revealed. Some of the earlier remarkable studies in this field have been the results of projects carried out within the German National Science Foundation (DFG). In these projects, the results of functionally modified coatings applied to optimize the thermal, wear and corrosion properties of metal and ceramic materials are outlined in the studies of [6,7]. Fundamental studies related to the production of FGMs, research of their thermo-mechanical properties, development of production techniques, manufacturing method and expansion of application areas continue until today [8–12]. The studies on the mechanical behavior of FGM coated sandwich construction elements in the literature started in 2005 with the initiative of Zenkour [13]. After this study, many studies on the static and dynamic behavior of plates and cylindrical shells containing FGM layers under different boundary conditions have been carried out using various theories and methods [14–36]. In addition, there are some alternative studies to solve many engineering problems including the theory of static and dynamic stability of neural networks models, associative memory, image and signal processing, optimization, pattern recognition, and others [37–40].

In most of the above studies, the stability and vibration problems of FG-coated sandwich structural members have been solved using either analytical methods for simply supported boundary conditions or numerical methods for various boundary conditions. The number of analytical solutions to the problems of stability and vibration of single-layer FG shells with clamped boundary conditions is limited. Among them, Shen et al. [41–43] use a singular perturbation technique to solve the buckling problems of single-layer FG cylindrical shells under clamped boundary conditions. Sofiyev et al. [44,45] solved the vibration and buckling problems of single-layer FG shells under clamped boundary conditions within the framework of classical theory. To obtain more realistic results in solving problems of stability and vibration of SCSs with FG-coatings under various boundary conditions, the developed theories should be used together with classical theories. Because FG-coated sandwich cylindrical shells are used in a variety of environments in industries that use advanced technologies, they operate in a variety of boundary conditions (free, freely-supported, simply-supported, etc.) as well as clamped boundary conditions. This situation requires the development of new solution methods for stability and vibration problems of clamped sandwich cylindrical shells coated with new generation heterogeneous composites (FGM) in the framework of the developed shell theories, which is very common in the nuclear, aerospace, aviation and automotive industries. The ability to put the problem of stability and vibration of FGM-coated sandwich cylinders with clamped edges, which is the scientific and technical problem, on a serious mathematical basis and their analytical solution by mathematical modeling, makes it possible to predict some design flaws and eliminate them. In this sense, this study is important and necessary.

The literature review reveals that no work has been done on the analytical solution of the vibration and stability problems of FG-coated SCSs with clamped edges under axial compressive load in the framework of STs. The aim of the study is to focus on the solution of this problem.

The remainder of the article is organized as follows. Mathematical modeling of the properties of sandwich cylindrical shells coated with FGM is performed in Section 2. The main relationships and equations within the framework of STs are given in Section 3. Analytical expressions for critical axial load and frequency are obtained in Section 4 using the Galerkin procedure. The accuracy of the methodology and original analyzes are presented in Section 5. The conclusion is drawn in Section 6.

2. Formulation of problem

2.1. Modeling of FG-coated sandwich cylindrical shells

Let's assume that the Oxy curvilinear coordinate system is selected at the lower left end of the reference surface of the core of the sandwich cylindrical shell with length$l$, radius$a$, and total thickness h subjected to the uniform axial load, T (Fig. 1):

$$N_{11}^0 = -T, \quad N_{22}^0 = N_{12}^0 = 0 \tag{1}$$

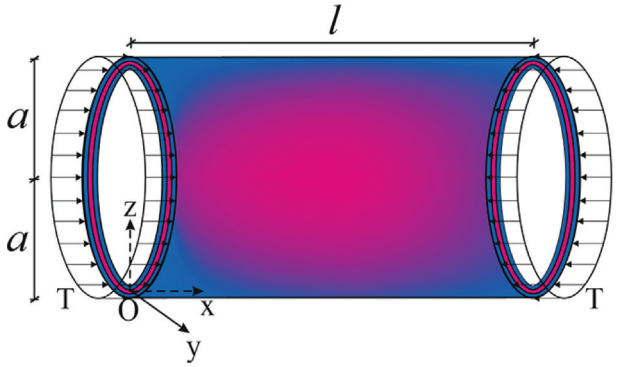


Fig. 1 Sandwich cylindrical shell under uniform axial load and coordinate system.

where $N_{ij}^{0}(i,j=1,2)$ represent forces for the initial torque-free state.

The Ox and Oy axes are in the longitudinal and circumferential directions, respectively, and the Oz axis is in the normal direction of the surface of the two axes. Six various types of SCSs are considered in this study (Figs. 2 and 3). Fig. 2 shows **a)** F_1-type coated shell with a ceramic-rich core or $F_1^{(1)}/C/F_1^{(3)}$ and cross section **b)** sandwich cylindrical shell with metal coatings (M/C/M) and cross section **c)** ceramic-rich (C/C/C) cylindrical shell and cross section [18]. The total thickness of the F_1-type coated shells with the ceramic-rich core is expressed as$h = 2h_{F_1} + h_c$. Here, the thickness of the core is h_c and the thickness of each coating is equal, denoted by h_{F_1}(Fig. 2a). The total thickness of the metal-coated shell with the ceramic-rich core is$h = 2h_m + h_c$. Here, the thickness of the core is h_c and the thickness of each metal coating is h_m (Fig. 2b).The total thickness of the cylindrical shell consisting of all three layers of the ceramic is $h = h_{c(1)} + h_{c(2)} + h_{c(3)}$ and presented in Fig. 2c.

In Fig. 3, **a)** F_2-type sandwich cylindrical shell or $F_2^{(1)}/M/F_2^{(3)}$ and cross section **b)** ceramic-coated sandwich cylindrical shell (C/M/C) and cross section c) metal-rich cylindrical shell (M/M/M) and cross section are presented [18]. The total thickness of the F_2-type coatings coated sandwich shells with the metal-rich core is expressed as$h = 2h_{F_2} + h_m$. Here, the thickness of the core is h_m and the thickness of each coating is equal, denoted by h_{F_2}(Fig. 3a). The total thickness of the ceramic-coated sandwich cylindrical shell with the metal-rich core is$h = 2h_c + h_m$. Here, the thickness of the core is h_m and the thickness of each ceramic coating is h_c(Fig. 3b). The total thickness of the cylindrical shell consisting of all three layers of the metal is $h = h_{m(1)} + h_{m(2)} + h_{m(3)}$ and presented in Fig. 3c.

2.2. Mathematical modeling of properties of sandwich cylindrical shells with homogeneous core and FG coatings

FGMs are formed from a mixture of metals and ceramics using different techniques, and their properties are defined by the following relationship [16–18]:

$$P = P_c V_c + P_m V_m \tag{2}$$

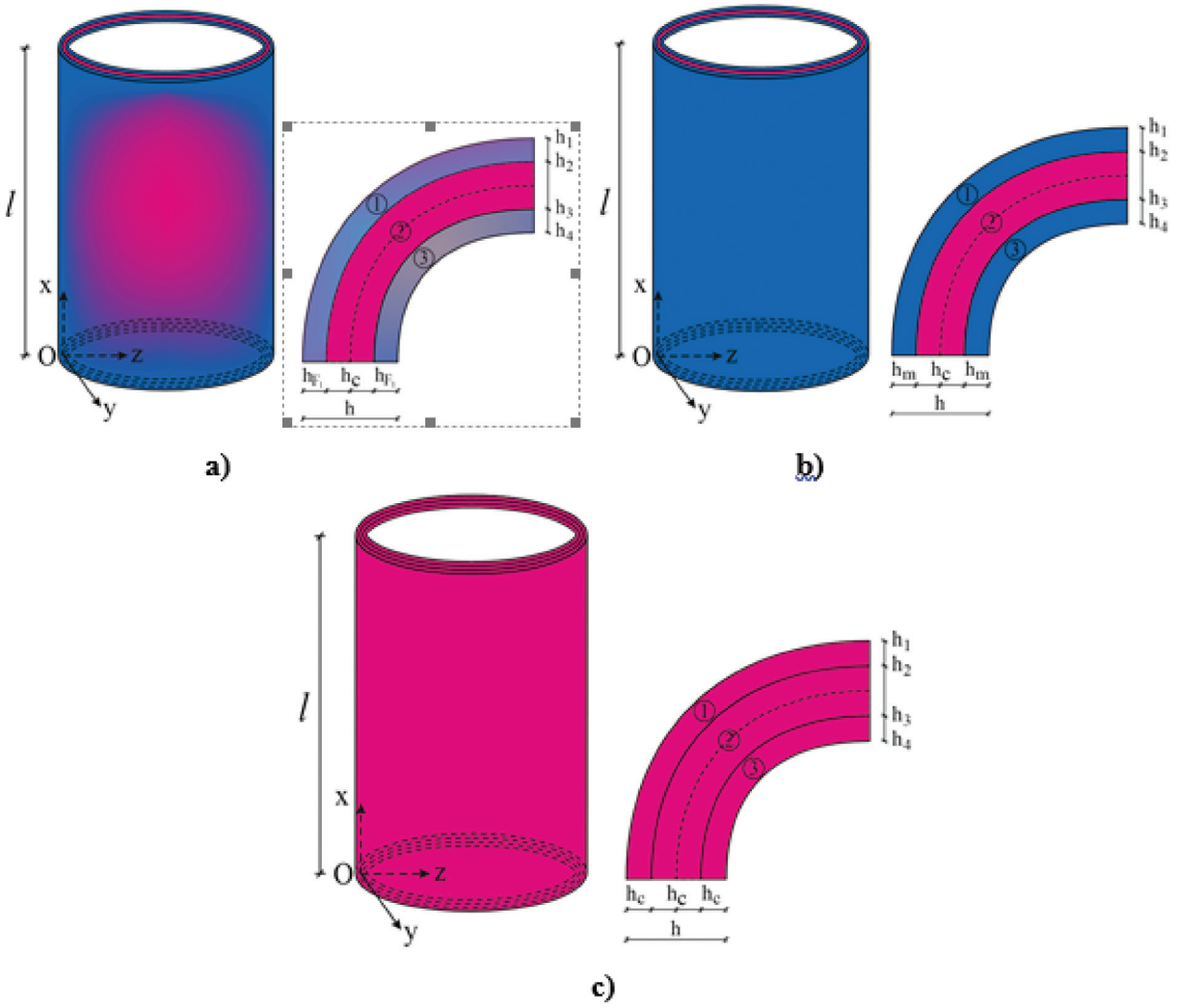


Fig. 2 **(a)** $F_1^{(1)}/C/F_1^{(3)}$-type cylinder with the ceramic-rich core and cross section **(b)** M/C/M−type cylinder and cross section **(c)** ceramic-rich cylinder and the cross section.

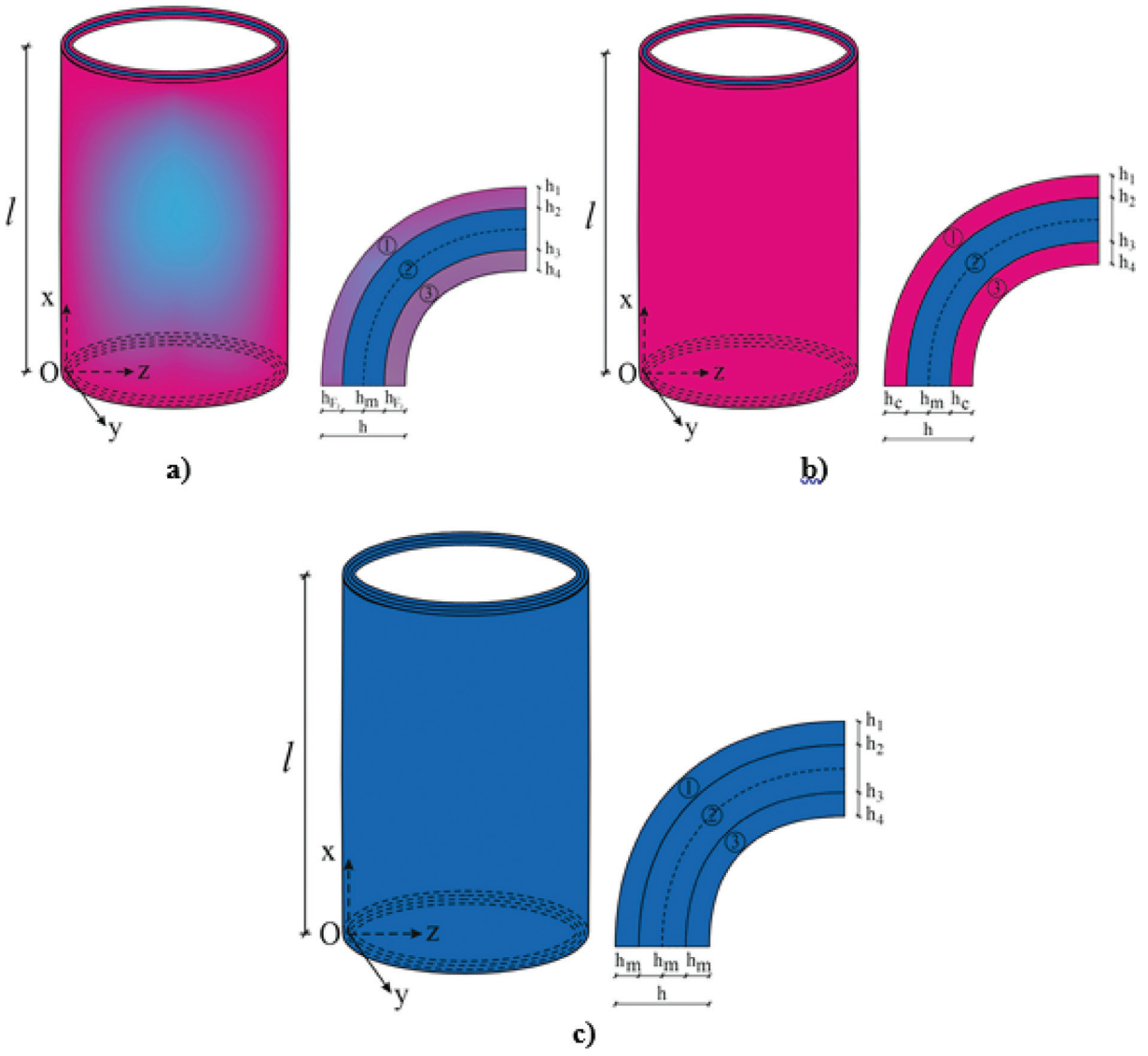


Fig. 3 **(a)** $F_2^{(1)}/M/F_2^{(3)}$-type cylinder with the metal-rich core and cross section **(b)** C/M/C-type cylinder and cross section **(c)** ceramic-rich cylindrical shell and cross section.

where P_c, P_m and V_c, V_m are the properties and volume fractions of the ceramic and metal surfaces of FGMs, respectively.

The properties of FG coatings are the function of temperature and are expressed as follows:

$$P = P_0 \sum_{i=-1}^{3} P_i T^i \tag{3}$$

where $P_i (i = -1, 0, ..., 3)$ are coefficients, T^i is the temperature dependent functions, expressed in Kelvin, and they are unique for material components [16–19].

It is assumed that the material properties of F_1 and F_2-type coatings gradually change from the outer surface to the inner surface in the z direction. In other words, the outer $(z = h_1 = -h/2)$ and inner $(z = h_4 = +h/2)$ surfaces of sandwich cylindrical shells are composed of FGMs, while the (h_2, h_3) surfaces are made of metal-rich or ceramic-rich. The volume fractions of F_1 and F_2-type coatings are the power function of the dimensionless variable $\bar{z}(= z/h)$, while the volume fraction of the core is equal to one. Therefore, the volume fractions of the layers forming the sandwich cylindrical shell are denoted by $V^{(k)} (k = 1, 2, 3)$, respectively, and expressed as follows [16–21]:

$$\begin{aligned} V^{(1)} &= \left(\frac{\bar{z}-z_1}{z_2-z_1}\right)^d, \qquad z_1 \leqslant \bar{z} < z_2, \qquad (z_1 = -0.5) \\ V^{(2)} &= \quad 1, \qquad\qquad z_2 \leqslant \bar{z} \leqslant z_3 \\ V^{(3)} &= \left(\frac{z_3-\bar{z}}{z_3-z_1}\right)^d, \qquad z_3 < \bar{z} \leqslant z_4 \qquad (z_4 = 0.5) \end{aligned} \tag{4}$$

where the vertical ordinates of the bottom, the two interfaces, and the top are denoted by $z_1 = h_1/h,\ z_2 = h_2/h,\ z_3 = h_3/h,\ z_4 = h_4/h$; d $(0 \leqslant d < +\infty)$ is the volume fraction index that determines the material change profile throughout the thickness of FG coatings.

$V_m^{(1)}$ and $V_m^{(3)}$ are the metal volume fractions of the coatings inside and outside the metal cylindrical shell, respectively, based on the relation (4) the following relations are valid:

$$V_m^{(k)} + V_c^{(k)} = 1, \ (k = 1, 3) \tag{5}$$

Using Eqs. (2) and (4), the Young's modulus, Poisson ratio and density of F_1 and F_2-type coatings on the inner and outer surfaces of sandwich shells are expressed as follows [16–21]:

$$\begin{aligned} &E_{F_1}^{(k)}(\bar{z}) = E_{\mathrm{m}} e^{V^{(k)} \ln(E_c/E_m)}, \quad v_{F_1}^{(k)}(\bar{z}) = v_{\mathrm{m}} e^{V^{(k)} \ln(v_c/v_m)}, \\ &\rho_{F_1}^{(k)}(\bar{z}) = \rho_{\mathrm{m}} e^{V^{(k)} \ln(\rho_c/\rho_m)} \\ &E_{F_2}^{(k)}(\bar{z}) = E_c e^{V^{(k)} \ln(E_m/E_c)}, \quad v_{F_2}^{(k)}(\bar{z}) = v_{\mathrm{c}} e^{V^{(k)} \ln(v_m/v_c)}, \\ &\rho_{F_2}^{(k)}(\bar{z}) = \rho_{\mathrm{c}} e^{V^{(k)} \ln(\rho_m/\rho_c)}, \ \mathrm{k} = 1, 3 \end{aligned} \tag{6}$$

where Young's modulus, Poisson's ratio and density of the metal and ceramic surfaces of F_1 and F_2-type coatings on the inner and outer surfaces of sandwich shells are defined as E_m, v_m, ρ_m andE_c, v_c, ρ_c, respectively.

Considering the relations (4)–(6), the expressions for the mechanical properties of sandwich shells covered by $F_i\,(i = 1, 2)$-type coatings; take the following form [18]:

$$\left[E(\bar{z}), v(\bar{z}), \rho(\bar{z})\right] = \begin{cases} E_{F_i}^{(1)}, v_{F_i}^{(1)}, \rho_{F_i}^{(1)} & z_1 \leqslant \bar{z} < z_2 \\ E_i^{(2)}, v_i^{(2)}, \ \rho_i^{(2)} & z_2 \leqslant \bar{z} \leqslant z_3 \\ E_{F_i}^{(3)}, v_{F_i}^{(3)}, \ \rho_{F_i}^{(3)} & z_3 < \bar{z} \leqslant z_4 \end{cases}, \ (i = 1, 2) \tag{7}$$

The volume fraction index of the $F_i^{(k)}(i = 1, 2; k = 1, 3)$–type coatings changes as$d = 0.5$, 1.0, 2.0. The dimensionless Young's modulus and dimensionless thickness coordinate are shown on the vertical and horizontal axes, respectively (see, Figs. 4 and 5). The variation of the dimensionless Young's modulus $(E(\bar{z})/E_c)$ of sandwich cylindrical shells with the ceramic-rich core and covered by $F_1^{(1)}$ and $F_1^{(3)}$-type coatings outside and inside, depending on the dimensionless thickness coordinate$\bar{z}$, is presented for different volume fraction indices in Fig. 4. The outer surface of the coating $F_1^{(1)}$-type consists of metal-rich and the volume fraction component gradually increases from the outer surface of the coating to the inner surface. On the inside surface is vice versa.

Similarly, the variation of the dimensionless Young's modulus $(E(\bar{z})/E_m)$ of sandwich cylindrical shells with the metal-rich core and covered by $F_2^{(1)}$ and $F_2^{(3)}$-type coatings outside and inside, depending on the $\bar{z}$ is presented in Fig. 5 for different volume fraction index. The outer surface of the coating $F_2^{(1)}$-type consists of ceramic-rich and the volume fraction component gradually decreases from the outer surface of the coating to the inner surface. On the inside surface is vice versa.

3. Basic relations

The constitutive relations for the k^{th} layer of FG-coated sandwich cylindrical shells in the framework of ST can be formed as follow [16–21,43]:

$$\begin{bmatrix} \sigma_{11}^{(k)} \\ \sigma_{22}^{(k)} \\ \sigma_{23}^{(k)} \\ \sigma_{13}^{(k)} \\ \sigma_{12}^{(k)} \end{bmatrix} = \begin{bmatrix} Q_{11i}^{(k)} & Q_{12i}^{(k)} & 0 & 0 & 0 \\ Q_{12i}^{(k)} & Q_{11i}^{(k)} & 0 & 0 & 0 \\ 0 & 0 & Q_{44i}^{(k)} & 0 & 0 \\ 0 & 0 & 0 & Q_{55i}^{(k)} & 0 \\ 0 & 0 & 0 & 0 & Q_{66i}^{(k)} \end{bmatrix} \begin{bmatrix} \varepsilon_{11} \\ \varepsilon_{22} \\ \gamma_{23} \\ \gamma_{13} \\ \gamma_{12} \end{bmatrix} \tag{8}$$

where $\sigma_{ij}^{(k)}(i = 1, 2, j = 1, 2, 3)$ are stresses in the k^{th} layer, $k(= 1, 2, 3)$ is the number of layers, $\varepsilon_{ii}(i = 1, 2)$, $\gamma_{ij}(i = 1, 2, \ j = 2, 3)$ are strains for sandwich cylindrical shells and $Q_{ij}^{(k)}(i, j = 1, 2, 6)$ represent material properties and defined as:

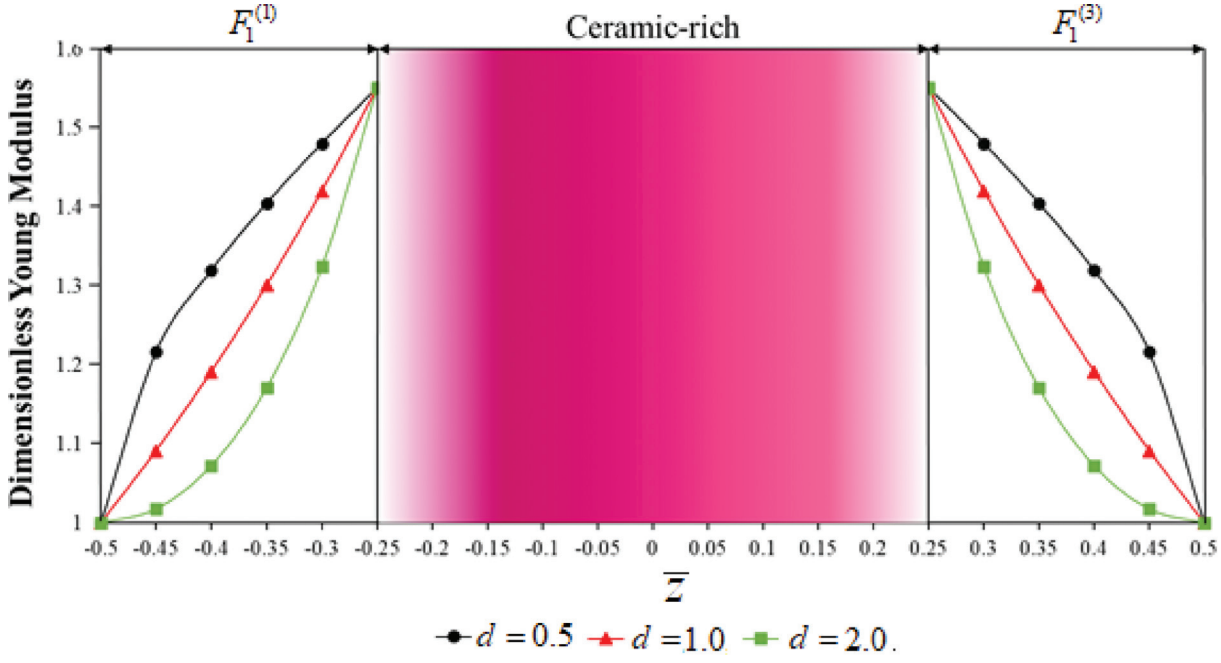


Fig. 4 Variation of dimensionless Young's modulus of sandwich shells with the ceramic-rich core and covered by F_1 -type coatings for different volume fraction indices.

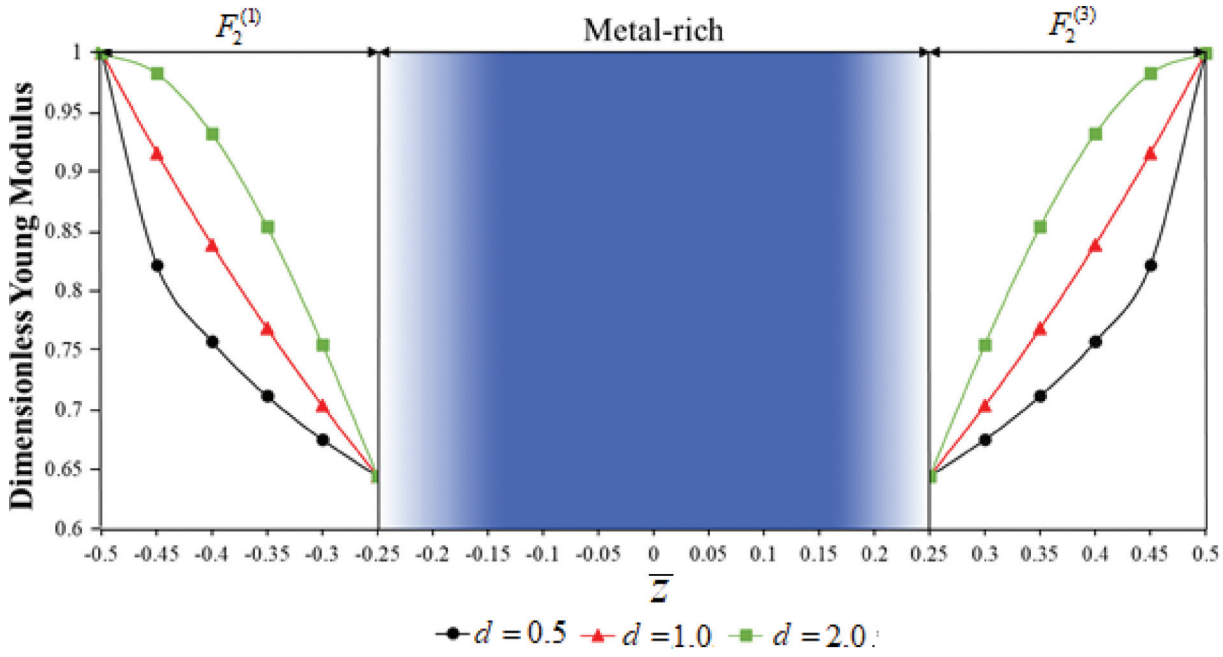


Fig. 5 Variation of dimensionless Young's modulus of sandwich shells with the metal-rich core and covered by F_2-type coatings for different volume fraction index.

$$Q_{11i}^{(k)}=\frac{E_{F_i}^{(k)}}{1-\left(\nu_{F_i}^{(k)}\right)^2},\quad Q_{12i}^{(k)}=\nu_{F_i}^{(k)}Q_{11i}^{(k)},$$
$$Q_{44i}^{(k)}=Q_{55i}^{(k)}=Q_{66i}^{(k)}=\frac{E_{F_i}^{(k)}}{2\left[1+\nu_{F_i}^{(k)}\right]},\ (k=1,3),$$
$$Q_{11i}^{(2)}=\frac{E_i^{(2)}}{1-\left(\nu_i^{(2)}\right)^2},\quad Q_{12i}^{(2)}=\nu_i^{(2)}Q_{11i}^{(2)},\quad Q_{44i}^{(2)}=Q_{55i}^{(2)}=Q_{66i}^{(2)}=\frac{E_i^{(2)}}{2\left[1+\nu_i^{(2)}\right]}. \tag{9}$$

Based on the STs, the transverse shear stresses (TSSs) in the k^{th} layer of FG-coated sandwich cylindrical shells vary in the thickness direction as follows [18]:

$$\sigma_{13}^{(k)}=\frac{df_1^{(k)}(z)}{dz}\varphi(x,y),\quad \sigma_{23}^{(k)}=\frac{df_2^{(k)}(z)}{dz}\psi(x,y),\ (k=1,2,3) \tag{10}$$

where $\varphi(x,y)$ and $\psi(x,y)$ are the rotation angle functions of the normal to the reference surface, $f_i^{(k)}(z)\,(i=1,2)$ are shear stress shape functions in the layers and their first-order derivatives determine the distribution of shear stresses $\sigma_{j3}^{(k)}(j=1,2)$ in the layers along the thickness direction.

Considering the relation (10) in the third and fourth equations of the system of Eqs (8), it turns into the following form:

$$\gamma_{13}=\frac{df_1^{(k)}(z)}{dz}a_{55i}^{(k)}(\bar{z})\varphi(x,y),\quad \gamma_{23}=\frac{df_2^{(k)}(z)}{dz}a_{44i}^{(k)}(\bar{z})\psi(x,y) \tag{11}$$

where

$$a_{55i}^{(k)}(\bar{z})=1/Q_{55i}^{(k)}(\bar{z}),\quad a_{44i}^{(k)}(\bar{z})=1/Q_{44i}^{(k)}(\bar{z}) \tag{12}$$

Based on the ST, the strains at a distance z from the reference surface of FG coated sandwich cylindrical shells are expressed as follows [18]:

$$\begin{pmatrix}\varepsilon_{11}\\ \varepsilon_{22}\\ \gamma_{12}\end{pmatrix}=\begin{pmatrix}\varepsilon_{11}^0-z\frac{\partial^2 w}{\partial x^2}+I_{1i}^{(k)}\frac{\partial\varphi}{\partial x}\\ \varepsilon_{22}^0-z\frac{\partial^2 w}{\partial y^2}+I_{2i}^{(k)}\frac{\partial\psi}{\partial y}\\ \gamma_{12}^0-2z\frac{\partial^2 w}{\partial x\partial y}+I_{1i}^{(k)}\frac{\partial\varphi}{\partial y}+I_{2i}^{(k)}\frac{\partial\psi}{\partial x}\end{pmatrix} \tag{13}$$

where $\varepsilon_{11}^0,\ \varepsilon_{22}^0,\ \gamma_{12}^0$ are the strains at the reference surface of FG sandwich cylindrical shells, and $I_{1i}^{(k)}$ and $I_{2i}^{(k)}$ are defined as follows:

$$I_{1i}^{(k)}=\int_0^z a_{55i}^{(k)}(\bar{z})\frac{df_1^{(k)}(z)}{dz}dz;$$
$$I_{2i}^{(k)}=\int_0^z a_{44i}^{(k)}(\bar{z})\frac{df_2^{(k)}(z)}{dz}dz,\ (k=1,2,3) \tag{14}$$

The force and moment components N_{ij} and $M_{ij}(i,j=1,2)$ of FG-coated sandwich cylindrical shells are found from the following integrals [43,46–48]:

$$\left(N_{ij},M_{ij}\right)=\sum_{k=1}^{3}\int_{h_k}^{h_{k+1}}(1,z)\sigma_{ij}^{(k)}dz \tag{15}$$

The shear force components $Q_i(i=1,2)$ of FG-coated sandwich cylindrical shells are found from the following integrals [43,46–48]:

$$(Q_1,Q_2)=\sum_{k=1}^{3}\int_{h_k}^{h_{k+1}}\left[\sigma_{13}^{(k)},\sigma_{23}^{(k)}\right]dz \tag{16}$$

The following relations are valid between the in-plane forces and the Airy stress function, Ψ [43,46–48]:

$$(N_{11},\ N_{22},\ N_{12})=h\left(\frac{\partial^2\Psi}{\partial y^2},\frac{\partial^2\Psi}{\partial x^2},-\frac{\partial^2\Psi}{\partial x\partial y}\right) \tag{17}$$

Substituting (10) into (16), gives the following expressions for shear forces:

$$Q_1=I_3\varphi,\quad Q_2=I_4\psi \tag{18}$$

where

$$I_3=\sum_{k=1}^{3}\int_{h_k}^{h_{k+1}}\frac{df_1^{(k)}(z)}{dz}dz,\ I_4=\sum_{k=1}^{3}\int_{h_k}^{h_{k+1}}\frac{df_2^{(k)}(z)}{dz}dz \tag{19}$$

Substituting the set of relations (13) into the set of constitutive equations (8) and then substituting the resulting expressions in the integrals (15) and taking into account the relations (17), the following expressions are obtained for the strains on the reference surface and moments for FG-coated sandwich cylindrical shells:

$$\begin{aligned}
\varepsilon_{11}^0&=B_1h\frac{\partial^2\Psi}{\partial y^2}+B_2h\frac{\partial^2\Psi}{\partial x^2}-B_3\frac{\partial^2 w}{\partial x^2}-B_4\frac{\partial^2 w}{\partial y^2}+B_7\frac{\partial\varphi}{\partial x}+B_8\frac{\partial\psi}{\partial y}\\
\varepsilon_{22}^0&=B_2h\frac{\partial^2\Psi}{\partial y^2}+B_1h\frac{\partial^2\Psi}{\partial x^2}-B_4\frac{\partial^2 w}{\partial x^2}-B_3\frac{\partial^2 w}{\partial y^2}+B_9\frac{\partial\varphi}{\partial x}+B_{10}\frac{\partial\psi}{\partial y}\\
\gamma_{12}^0&=-B_5h\frac{\partial^2\Psi}{\partial x\partial y}-B_6\frac{\partial^2 w}{\partial x\partial y}-B_{11}\frac{\partial\varphi}{\partial y}-B_{12}\frac{\partial\psi}{\partial x}
\end{aligned} \tag{20}$$

and

$$\begin{aligned}
M_{11}&=C_1h\frac{\partial^2\Psi}{\partial y^2}+C_2h\frac{\partial^2\Psi}{\partial x^2}-C_3\frac{\partial^2 w}{\partial x^2}-C_4\frac{\partial^2 w}{\partial y^2}+C_7\frac{\partial\varphi}{\partial x}+C_8\frac{\partial\psi}{\partial y}\\
M_{22}&=C_2h\frac{\partial^2\Psi}{\partial y^2}+C_1h\frac{\partial^2\Psi}{\partial x^2}-C_4\frac{\partial^2 w}{\partial x^2}-C_3\frac{\partial^2 w}{\partial y^2}+C_9\frac{\partial\varphi}{\partial x}+C_{10}\frac{\partial\psi}{\partial y}\\
M_{12}&=-C_5h\frac{\partial^2\Psi}{\partial x\partial y}-C_6\frac{\partial^2 w}{\partial x\partial y}-C_{11}\frac{\partial\varphi}{\partial y}-C_{12}\frac{\partial\psi}{\partial x}
\end{aligned} \tag{21}$$

where B_{ij} and C_{ij} are given in Appendix A.

4. Basic equations

Based on the STs, the dynamic stability equations of FG-coated sandwich cylindrical shells are as follows [18,43,46–48]:

$$\begin{aligned}
&\frac{\partial M_{11}}{\partial x}+\frac{\partial M_{12}}{\partial y}-Q_1=0,\ \frac{\partial M_{21}}{\partial x}+\frac{\partial M_{22}}{\partial y}-Q_2=0\\
&\frac{\partial^2\varepsilon_{11}^0}{\partial y^2}+\frac{\partial^2\varepsilon_{22}^0}{\partial x^2}-\frac{\partial^2\gamma_{12}^0}{\partial x\partial y}+\frac{1}{a}\frac{\partial^2 w}{\partial x^2}=0\\
&\frac{\partial Q_1}{\partial x}+\frac{\partial Q_2}{\partial y}+\frac{N_{22}}{a}+N_{11}^0\frac{\partial^2 w}{\partial x^2}+2N_{12}^0\frac{\partial^2 w}{\partial x\partial y}+N_{22}^0\frac{\partial^2 w}{\partial y^2}-\rho_t\frac{\partial^2 w}{\partial t^2}=0
\end{aligned} \tag{22}$$

where N_{ij}^0 are the pre-buckling forces which $N_{11}^0=-T$, $N_{12}^0=N_{22}^0=0$ and t is the time parameter and the following definitions apply:

$$\rho_t=\int_{-h/2}^{-h_2}\rho_{F_i}^{(1)}dz+\rho_i^{(2)}(h_2+h_3)+\int_{h_3}^{h/2}\rho_{F_i}^{(3)}dz,\ (i=1,2) \tag{23}$$

By substituting relations (17), (18), (20) and (21) into equations (22), after some mathematical operations, the dynamic stability and compatibility equations of FGM coated sandwich cylindrical shells under axial compressive load, take the form of the following matrix equation:

$$\begin{bmatrix}L_{11}&L_{12}&L_{13}&L_{14}\\L_{21}&L_{22}&L_{23}&L_{24}\\L_{31}&L_{32}&L_{33}&L_{34}\\L_{41}&L_{42}&L_{43}&L_{44}\end{bmatrix}\begin{bmatrix}\Psi\\w\\\varphi\\\psi\end{bmatrix}=0 \tag{24}$$

where $L_{ij}(i,j=1,2,..,4)$ are differential operators and defined as:

$$\begin{aligned}
L_{11}&=(C_1-C_5)h\frac{\partial^4}{\partial x^2\partial y^2}+C_2h\frac{\partial^4}{\partial x^4},\\
L_{12}&=-C_3\frac{\partial^4}{\partial x^4}-(C_4+C_6)\frac{\partial^4}{\partial x^2\partial y^2},\\
L_{13}&=C_7\frac{\partial^3}{\partial x^3}+C_{11}\frac{\partial^3}{\partial x\partial y^2}-I_3\frac{\partial}{\partial x},\ L_{14}=(C_8+C_{12})\frac{\partial^3}{\partial x^2\partial y},\\
L_{21}&=C_2h\frac{\partial^4}{\partial y^4}+(C_1-C_5)h\frac{\partial^4}{\partial x^2\partial y^2},\\
L_{22}&=-(C_6+C_4)\frac{\partial^4}{\partial x^2\partial y^2}-C_3\frac{\partial^4}{\partial y^4},L_{23}=(C_9+C_{11})\frac{\partial^3}{\partial x\partial y^2},\\
L_{24}&=C_{10}\frac{\partial^3}{\partial y^3}+C_{12}\frac{\partial^3}{\partial x^2\partial y}-I_4\frac{\partial}{\partial y},\\
L_{31}&=B_1h\frac{\partial^4}{\partial x^4}+(2B_2+B_5)h\frac{\partial^4}{\partial x^2\partial y^2}+B_1h\frac{\partial^4}{\partial y^4},\\
L_{33}&=B_9\frac{\partial^3}{\partial x^3}+(B_7+B_{11})\frac{\partial^3}{\partial x\partial y^2},\\
L_{32}&=\frac{1}{a}\frac{\partial^2}{\partial x^2}-B_4\frac{\partial^4}{\partial x^4}-(2B_3-B_6)\frac{\partial^4}{\partial x^2\partial y^2}-B_4\frac{\partial^4}{\partial y^4},\\
L_{34}&=(B_{10}+B_{12})\frac{\partial^3}{\partial x^2\partial y}+B_8\frac{\partial^3}{\partial y^3},\\
L_{41}&=\frac{h}{a}\frac{\partial^2}{\partial x^2},\ L_{42}=-T\frac{\partial^2}{\partial x^2}-\rho_t\frac{\partial^2}{\partial t^2},\ L_{43}=I_3\frac{\partial}{\partial x},\ L_{44}=I_4\frac{\partial}{\partial y}.
\end{aligned} \tag{25}$$

If TSSs are not taken into account in the basic relationships, the basic equations of sandwich cylindrical shells with FG coatings in the CT frame take the following form [15]:

$$\begin{bmatrix}L_{11}&L_{12}\\L_{21}&L_{22}\end{bmatrix}\begin{bmatrix}\Psi\\w\end{bmatrix}=0 \tag{26}$$

where $L_{ij}(i,j=1,2)$ are differential operators and are defined as:

$$\begin{aligned}
L_{11}&=C_2h\frac{\partial^4}{\partial x^4}+2h(C_1-C_5)\frac{\partial^4}{\partial x^2\partial y^2}+C_2h\frac{\partial^4}{\partial y^4}+\frac{h}{a}\frac{\partial^2}{\partial x^2},\\
L_{12}&=-C_3\frac{\partial^4}{\partial x^4}-2(C_4+C_6)\frac{\partial^4}{\partial x^2\partial y^2}-C_3\frac{\partial^4}{\partial y^4}-T\frac{\partial^2}{\partial x^2}-\rho_t\frac{\partial^2}{\partial t^2},\\
L_{21}&=B_1h\frac{\partial^4}{\partial x^4}+h(2B_2+B_5)\frac{\partial^4}{\partial x^2\partial y^2}+hB_1\frac{\partial^4}{\partial y^4},\\
L_{22}&=-B_4\frac{\partial^4}{\partial x^4}-(2B_3-B_6)\frac{\partial^4}{\partial x^2\partial y^2}-B_4\frac{\partial^4}{\partial y^4}+\frac{1}{a}\frac{\partial^2}{\partial x^2}.
\end{aligned} \tag{27}$$

5. Solution procedure

Let's assume that the two edges of the sandwich cylindrical shell with FG coatings to be clamped, so that the boundary conditions are [41–43]:

$$w=0,\quad v=0,\ \varphi=0,\quad \psi=0,\ \text{as } x=0 \text{ and } x=l \tag{28a}$$

$$\int_0^{2\pi a}N_{11}\mathrm{d}y+2\pi\mathrm{a}T=0 \tag{28b}$$

The solution of the system of equations (24) is sought as the following new approximation functions:

$$\begin{aligned}
\Psi(x,y,t)&=\bar{\Psi}(t)\ \sin^2(\alpha x)\ \sin(\beta y),\\
w(x,y,t)&=\bar{w}(t)\sin^2(\alpha x)\ \sin(\beta y),\\
\varphi(x,y,t)&=\bar{\varphi}(t)\cos\ (\alpha x)\sin(\alpha x)\sin(\beta y),\\
\psi(x,y,t)&=\bar{\psi}(t)\sin^2(\alpha x)\ \cos(\beta y)
\end{aligned} \tag{29}$$

where $\alpha=\frac{m\pi}{l}$ and $\beta=\frac{n}{a}$ are parameters that depend on the length and radius of the FG sandwich shells, and m and n wave numbers.

Substituting expressions (29) into the equations set of (24), and then applying the Galerkin procedure, it reduces to the following equations:

$$
\begin{aligned}
&K_{C11}\,\bar{\Psi}(t)-K_{C12}\,\bar{w}(t)+K_{C13}\,\bar{\varphi}(t)+K_{C14}\,\bar{\psi}(t)=0\\
&K_{C21}\,\bar{\Psi}(t)-K_{C22}\,\bar{w}(t)+K_{C23}\,\bar{\varphi}(t)+K_{C24}\,\bar{\psi}(t)=0\\
&K_{C31}\,\bar{\Psi}(t)-K_{C32}\,\bar{w}(t)+K_{C33}\,\bar{\varphi}(t)+K_{C34}\,\bar{\psi}(t)=0\\
&K_{C41}\,\bar{\Psi}(t)+\left[K_{C\rho_t}\tfrac{\mathrm{d}^2}{\mathrm{dt}^2}-K_{Cax}T\right]\bar{w}(t)+K_{C43}\,\bar{\varphi}(t)+K_{C44}\,\bar{\psi}(t)=0
\end{aligned}
\tag{30}
$$

where $K_{Cij}(i=1,2,...,4)$ are the parameters that include the properties of FG coating sandwich cylindrical shells with the clamped edges, $K_{C\rho_t}$ and K_{Cax} are the coefficients characterizing the density and axial compressive load, respectively, and their contents are shown below:

$$
\begin{aligned}
&K_{C11}=\alpha^2\beta^2(C_1-C_5)h+4\alpha^4c_{12}h,\\
&K_{C12}=4\alpha^4C_3+\alpha^2\beta^2(C_4+C_6),\\
&K_{C13}=2C_7\alpha^3+\tfrac{1}{2}\alpha\beta^2C_{11}+\tfrac{1}{2}\alpha I_3,\\
&K_{C14}=\alpha^2\beta(C_8+C_{12}),\\
&K_{C21}=4\alpha^2C_2h+\alpha^2\beta^2h(C_1-C_5),\\
&K_{C22}=\tfrac{3}{4}C_3\beta^4+(C_4+C_6)\alpha^2\beta^2,\\
&K_{C23}=\tfrac{1}{2}\alpha\beta^2(C_9+C_{11}),\\
&K_{C24}=\tfrac{3}{4}\beta I_4+\tfrac{3}{4}\beta^3C_{10}+C_{12}\alpha^2\beta,\\
&K_{C31}=h\left(4\alpha^4+\tfrac{3}{4}\beta^4\right)B_1+h\alpha^2\beta^2(B_5+2B_2),\\
&K_{C32}=(2B_3-B_6)\alpha^2\beta^2+\tfrac{3B_4}{4}\beta^4+\tfrac{1}{a}\alpha^2+4B_4\alpha^4,\\
&K_{C33}=2B_9\alpha^3+\tfrac{1}{2}(B_7+B_{11})\beta^2\alpha,\\
&K_{C34}=\tfrac{3}{4}B_8\beta^3+(B_{10}+B_{12})\alpha^2\beta,\\
&K_{C41}=\tfrac{h\alpha^2}{a},K_{C43}=\tfrac{1}{2}I_3\beta,\\
&K_{C44}=\tfrac{3}{4}I_4\beta,K_{Cax}=\alpha^2,\ K_{C\rho_t}=\tfrac{3}{4}\rho_t.
\end{aligned}
\tag{31}
$$

After removing the variables $\bar{\Psi}(t)$, $\bar{\varphi}(t)$, $\bar{\psi}(t)$ from the system of Eqs. (30), it turns into the following time-dependent second-order ordinary differential equation after some mathematical operations:

$$
K_{C\rho_t}\frac{d^2\bar{w}(t)}{dt^2}+(\Gamma_{ST}-K_{Cax}T)\,\bar{w}(t)=0 \tag{32}
$$

where

$$
\Gamma_{ST}=\frac{Y_{C22}Y_{C11}-Y_{C12}Y_{C21}}{Y_{C11}} \tag{33}
$$

in which

$$
\begin{aligned}
&Y_{C11}=X_{C21}-\tfrac{X_{C11}X_{C23}}{X_{C13}},\quad Y_{C12}=X_{C22}-\tfrac{X_{C12}X_{C23}}{X_{C13}},\\
&Y_{C21}=X_{C31}-\tfrac{X_{C11}X_{C33}}{X_{C13}},\\
&Y_{C22}=X_{C32}-\tfrac{X_{C12}X_{C23}}{X_{C13}},X_{C11}=K_{C21}-\tfrac{K_{C11}K_{C24}}{K_{C14}},\\
&X_{C12}=\tfrac{K_{C12}K_{C24}}{K_{C14}}-K_{C22},\\
&X_{C13}=K_{C23}-\tfrac{K_{C24}K_{C13}}{K_{C14}},\ X_{C21}=K_{C31}-\tfrac{K_{C11}K_{C34}}{K_{C14}},\\
&X_{C22}=\tfrac{K_{C12}K_{C34}}{K_{C14}}-K_{C32},\\
&X_{C23}=K_{C33}-\tfrac{K_{C13}K_{C34}}{K_{C14}},\ X_{C31}=K_{C41}-\tfrac{K_{C11}K_{C44}}{K_{C14}},\\
&X_{C32}=\tfrac{K_{C12}K_{C44}}{K_{C14}},\quad X_{C33}=K_{C43}-\tfrac{K_{C13}K_{C44}}{K_{C14}}.
\end{aligned}
\tag{34}
$$

Eq. (32) is the dynamic stability equation of clamped sandwich cylindrical shells covered by FG-coatings under the axial compressive load in the framework of STs.

Ignoring the axial load term from Eq. (32), the frequency of clamped sandwich cylindrical shells covered by FG coatings within STs is found from the following expression:

$$
\Omega_{ST}^{CC}=\sqrt{\frac{\Gamma_{ST}}{K_{C\rho_t}}} \tag{35}
$$

The following expression is used for dimensionless frequency parameter based on STs:

$$
\Omega_{1ST}^{CC}=\Omega_{ST}^{CC}a\sqrt{\frac{\rho_c(1-\nu_c^2)}{E_c}} \tag{36}
$$

Ignoring the inertia term from Eq. (32), the following expression is obtained for the dimensionless critical axial compressive load of the clamped sandwich cylindrical shells covered by FG coatings within STs:

$$
T_{1STcr}^{CCax}=\frac{1}{E_ch}\frac{\Gamma_{ST}}{K_{Cax}} \tag{37}
$$

It should be emphasized that it will be sufficient to use the first two functions in (29) for the solution of equation (26). Substituting these functions into the set of Eqs. (26), and then applying the Galerkin method, it turns into the following ordinary differential equation:

$$
\begin{aligned}
&\tfrac{d^2\bar{w}(t)}{dt^2}+\tfrac{8}{3\rho_t}\Bigg\{2C_3\alpha^4+\alpha^2\beta^2(C_4+C_6)+\tfrac{3}{8}C_3\beta^4\\
&\quad-\left[2C_2\alpha^4+\alpha^2\beta^2(C_1-C_5)+\tfrac{3}{8}C_2\beta^4-\tfrac{1}{2}\tfrac{\alpha^2}{a}\right]\\
&\times\frac{2B_4\alpha^4+\frac{1}{2}\alpha^2\beta^2(2B_3-B_6)+\frac{3}{8}B_4\beta^4+\frac{1}{2}\frac{\alpha^2}{a}}{2B_1\alpha^4+\frac{1}{2}\alpha^2\beta^2(2B_2+B_5)+\frac{3}{8}B_1\beta^4}-\frac{1}{2}T\alpha^2\Bigg\}\bar{w}(t)=0
\end{aligned}
\tag{38}
$$

Ignoring the axial load term from Eq. (38), the dimensionless frequency parameter of the clamped sandwich cylindrical shells covered by FG coatings in the framework of the CT is found from the following expression:

$$
\Omega_{1CT}^{CC}=a\sqrt{\frac{\rho_c(1-\nu_c^2)}{\rho_tE_c}\Gamma_{CT}} \tag{39}
$$

where

$$
\begin{aligned}
\Gamma_{CT}=\tfrac{1}{3}\Big\{&16C_3\alpha^4+8\alpha^2\beta^2(C_4+C_6)+3C_3\beta^4\\
&+\left[\tfrac{4\alpha^2}{a}-16C_2\alpha^4-8\alpha^2\beta^2(C_1-C_5)\right.\\
&\left.-3C_2\beta^4\right]\times\frac{16B_4\alpha^4+4\alpha^2\beta^2(2B_3-B_6)+3B_4\beta^4+\frac{4\alpha^2}{a}}{16B_1\alpha^4+4\alpha^2\beta^2(2B_2+B_5)+3B_1\beta^4}\Big\}
\end{aligned}
\tag{40}
$$

Ignoring the inertia term from the Eq. (38), the following expression is obtained for the dimensionless critical axial compressive load of the clamped sandwich cylindrical shells covered by FG-coating based on CT:

$$
\mathrm{T}_{1CTcr}^{CCax}=\frac{\Gamma_{CT}}{4\alpha^2E_ch} \tag{41}
$$

To obtain similar expressions for single-walled FG cylindrical shells, the following expressions are used instead of (4)–(6):

$V_c=\left(\bar{z}+0.5\right)^d,\ -0.5\leqslant\bar{z}<0.5,\qquad E_F(\bar{z})=E_{\mathrm{m}}e^{V_c\ln(E_c/E_{\mathrm{m}})},$

$\nu_F(\bar{z})=\nu_{\mathrm{m}}e^{V_c\ln(\nu_c/\nu_{\mathrm{m}})},\qquad \rho_F(\bar{z})=\rho_{\mathrm{m}}e^{V_c\ln(\nu_c/\nu_{\mathrm{m}})}$

and $\left[E(\bar{z}),\nu(\bar{z}),\rho(\bar{z})\right]=[E_F,\nu_F,\rho_F]$.

Table 1 Comparison of the lowest values of the Ω_{1CT}^{CC} and f (in Hz) for the homogeneous isotropic single-layer cylindrical shell with clamped edges.

$\Omega_{1CT}^{CC}=\Omega a\sqrt{(1-v_{0m}^2)\rho_{0m}/E_{0m}}$		
Loy et al. [49]	Zhang et al. [50]	Present study
0.01393(1,2)	0.01405(1,2)	0.01401(1,2)
$f=\Omega_{CT}^{CC}/2\pi$ (Hz)		
Zhang et al. [50] FEM	Zhang et al. [50]	Present study
12.25(1,1)	12.17(1,1)	12.084(1,1)

In order to find the minimum values of dimensionless frequency parameter and critical axial load of FG coated sandwich shells with clamped edges within CT and ST, the obtained expressions are minimized according to the wave numbers (m, n).

6. Discussion and results

6.1. Comparison examples

In this subsection, numerical calculations are performed to test the analytical expressions for the frequency parameter and the critical axial load. The numerical results are compared with those published in the literature using the Maple 14 software. The comparison of the minimum magnitudes of the frequency parameter,Ω_{1CT}^{CC} and cyclic frequency $f=\Omega_{CT}^{CC}/2\pi$ (in Hz) for the homogeneous isotropic single-layer cylindrical shell under clamped boundary conditions with those of Loy et al. [49] and Zhang et al. [50] are given in Table 1. The following data are used in the comparisons [49]: $E_{0m}=2.1\text{GPa}$, $v_{0m}=0.3$, $\rho_{0m}=7850\,\text{kg/m}^3, l/a=20,\ h/a=0.01$ As can be seen from Table 1, our results are in good agreement with those of Loy et al [49] and Zhang et al. [50].

The magnitudes of the cyclic frequency, $f=\Omega_{CT}^{CC}/2\pi$ (Hz) for homogeneous three-layered cylindrical shells with clamped edges are compared in Table 2 with the solution of Lam and Loy [45] for differentl/a. The material properties of the inner and outer layers of sandwich homogenous cylindrical shells are:$E_0^{(k)}=4.8265$ GPa, $v_0^{(k)}=0.3$ and$\rho_0^{(k)}=1314\,\text{kg/m}^3$ (k = 1, 3). The material properties of the coreare: $E_0^{(2)}=206.85$ GPa, $v_0^{(2)}=0.3$ and$\rho_0^{(2)}=8053\ \text{kg/m}^3$. The geometric characteristics of three-layered cylindrical shell are as follows: $h_i=0.0008$ m (i = 1, 3), $h_2=h_i/2, a=1\,\text{m}$, a/h = 500, m = 1.

Table 2 Comparison of the values of $f=\Omega_{CT}^{CC}/2\pi$ (Hz) for the homogeneous three-layered cylindrical shell with clamped edges for differentl/a.

$f=\Omega_{CT}^{CC}/2\pi$ (Hz), (n)		
l/a	Lam and Loy [51]	Present study
1.0	63.471(17)	62.741 (14)
2.0	32.525(13)	31.416 (10)
5.0	13.122(8)	12.724 (7)
20	3.1753(4)	3.245(3)

The comparisons show that the values of the cyclic frequency are in good agreement with those of Lam and Loy [51].

6.2. Typical numerical calculations and analysis

In this subsection, the values of dimensionless frequency parameters and critical axial load of sandwich cylindrical shells with FG coatings under clamped edges are found numerically in the framework of CT and ST. The obtained results are analyzed for different shear stress functions and for various coating types. The expressions (35)–(37), (39) and (41) are used to create the following tables and plot the graphs.

It is assumed that the shear stress functions vary as parabolic $f_i^{(k)}(z)=z\left(1-4z^2/3h^2\right)$, uniform$f_i^{(k)}(z)=z$, and cosine-hyperbolic $f_i^{(k)}(z)=h\sin(z/h)-z\cosh(1/2)$, $(i=1,2)$ [43,46,48]. For clarity, in the next steps we will denote the parabolic shear stress function as Par-SSF, the cosine-hyperbolic parabolic shear stress function as Cos-Hyp-SSF, and the uniform parabolic shear stress function as U-SSF. In numerical analysis, a mixture of stainless steel and silicon nitrate, SUS304/Si_3N_4 or $F_i^{(k)}(i=1,2;\ k=1,3)$ are used as FG coatings:$F_1^{(1)}/Si_3N_4/F_1^{(3)}$ or$F_1^{(1)}/C/F_1^{(3)}$, and $F_2^{(1)}/SUS304/F_2^{(3)}$ or$F_2^{(1)}/M/F_2^{(3)}$. In numerical analysis, the material properties of metal-rich (SUS304), ceramic-rich (Si_3N_4) and $F_i^{(k)}(i=1,2;\ k=1,3)$ type coatings are presented in Table 3 for $T(K)=300\text{K}$[43].

The variation ofT_{1STcr}^{CCax},T_{1CTcr}^{CCax},Ω_{1ST}^{CC} and Ω_{1CT}^{CC} values of M/C/M,$F_1^{(1)}/C/F_1^{(3)}$, C/M/C, $F_2^{(1)}/M/F_2^{(3)}$ sandwich, ceramic-rich and metal-rich monolayer cylindrical shells depending on the a/h ratio is presented in Tables 4 and 5 using three different SSFs. Geometric dimensions and volume fraction index of sandwich cylindrical shells are used as follows:$l/a=0.5$, $h_c/h_{coat}=4$ and $d=1$.Tables 4 and 5 show that the magnitudes of critical parameters of sandwich cylindrical shells with metal and ceramic-rich cores decrease due to the increase of the a/h ratio, while the number of transverse wave numbers increases. If the critical axial loads for $F_1^{(1)}/C/F_1^{(3)}$ and $F_2^{(1)}/M/F_2^{(3)}$ shells are compared among themselves, the critical axial load or dimensional frequency parameter of $F_1^{(1)}/C/F_1^{(3)}$ shells higher than $F_2^{(1)}/M/F_2^{(3)}$ *for* the small values ofa/h, while this difference decreases as the a/h incement. The effects of F_1 and F_2-type coatings on the dimensionless critical axial load (or dimensionless frequency parameter) are the same for Par- and Cos-Hyp-SSFs, while those are differ for the U-SSF. In all three STs, the effects of functionally graded coatings on critical parameters are significant. For example, in the Par- and Cos-Hyp-SSFs, when the $F_1^{(1)}/C/F_1^{(3)}$ and $F_2^{(1)}/M/F_2^{(3)}$ sandwich shells are compared with M/C/M and C/M/C sandwich shells, the effects of F_1 and F_2-type coatings on the dimensionless critical axial load decrease from (+16.54 %) to (+12 %) and from (−16.55 %) to (−12.34 %), respectively, whereas, those effects on the dimensionless frequency parameter decrease from (+31.94 %) to (+29.34 %) and from (−17.23 %) to (−15.15 %), respectively, as a/h increases from 20 to 75. When comparing $F_1^{(1)}/C/F_1^{(3)}$ shells with the single-layer C/C/C shell, the effects on the dimensionless critical axial load and dimensionless frequency parameter decrease from (−15.1 %) to (-13.8 %) and from (−24.46 %) to

Table 3 Temperature dependent coefficients of Young moduli (Pa), Poisson ratios and densities (kg/m^3) of ceramics and metals.

Young Moduli	E_0	E_{-1}	E_1	E_2	E_3	E_f
Silicon nitrate (Si_3N_4)	3.4843×10^{11}	0	-3.070×10^{-4}	2.160×10^{-7}	-8.946×10^{-11}	3.22271×10^{11}
Stainless steel (SUS304)	2.0104×10^{11}	0	3.079×10^{-4}	-6.534×10^{-7}	0	2.07788×10^{11}
Poisson ratios	ν_0	ν_{-1}	ν_1	ν_2	ν_3	ν_f
Silicon nitrate (Si_3N_4)	0.24	0	0	0	0	0.24
Stainless steel (SUS304)	0.3262	0	-2.002×10^{-4}	3.797×10^{-7}	0	0.317756
Densities	ρ_0	ρ_{-1}	ρ_1	ρ_2	ρ_3	ρ_f
Silicon nitrate (Si_3N_4)	2370	0	0	0	0	2370
Stainless steel (SUS304)	8166	0	0	0	0	8166

Table 4 Variation of T_{1STcr}^{CCax} and T_{1CTcr}^{CCax} for clamped sandwich and monolayer cylindrical shells depending on the a/h for three different SSFs.

	$T_{1STcr}^{CCax} \times 10^2$ (n_{cr})	$T_{1CTcr}^{CCax} \times 10^2$ (n_{cr})	$T_{1STcr}^{CCax} \times 10^2$ (n_{cr})	$T_{1CTcr}^{CCax} \times 10^2$ (n_{cr})	$T_{1STcr}^{CCax} \times 10^2$ (n_{cr})	$T_{1CTcr}^{CCax} \times 10^2$ (n_{cr})
	$M/C/M$		$F_1^{(1)}/C/F_1^{(3)}$		$C/C/C$	
a/h	$f_{i,z}^{(k)} = cosh(\bar{z}) - cosh(1/2)$ and $f_{i,z}^{(k)} = 1 - 4\bar{z}^2$ $(i = 1,2,\ k = 1,2,3)$					
20	2.788 (1)	3.048 (1)	3.249 (1)	3.455 (1)	3.827 (1)	4.161 (1)
30	1.586 (1)	1.641 (1)	1.808 (1)	1.850 (1)	2.127 (1)	2.197 (1)
50	0.906(3)	0.913(3)	1.017(3)	1.023(3)	1.180 (2)	1.189 (2)
75	0.608(6)	0.610(6)	0.681(6)	0.683(6)	0.790 (6)	0.793 (6)
a/h	$f_{i,z}^{(k)} = 1$					
20	2.827 (1)	3.048 (1)	3.275 (1)	3.455 (1)	3.879 (1)	4.161 (1)
30	1.595 (1)	1.641 (1)	1.813 (1)	1.850 (1)	2.138 (1)	2.197 (1)
50	0.907(3)	0.914(3)	1.017(3)	1.023(3)	1.181 (2)	1.189 (2)
75	0.608 (6)	0.610 (6)	0.681(6)	0.683(6)	0.790 (6)	0.793 (6)
	$C/M/C$		$F_2^{(1)}/M/F_2^{(3)}$		$M/M/M$	
a/h	$f_{i,z}^{(k)} = cosh(\bar{z}) - cosh(1/2)$ and $f_{i,z}^{(k)} = 1 - 4\bar{z}^2$ $(i = 1,2,\ k = 1,2,3)$					
20	3.583 (1)	3.907 (1)	2.990 (1)	3.415 (1)	2.544 (1)	2.793 (1)
30	1.955 (1)	2.023 (1)	1.679 (1)	1.770 (1)	1.413 (1)	1.465 (1)
50	1.049 (1)	1.058 (1)	0.916 (1)	0.929 (1)	0.778 (2)	0.785 (2)
75	0.704 (5)	0.706 (5)	0.617 (6)	0.620 (5)	0.521 (6)	0.524 (6)
a/h	$f_{i,z}^{(k)} = 1$					
20	3.633 (1)	3.907 (1)	3.065 (1)	3.415 (1)	2.582 (1)	2.793 (1)
30	1.966 (1)	2.023 (1)	1.696 (1)	1.770 (1)	1.421 (1)	1.465 (1)
50	1.050 (1)	1.058 (1)	0.919 (1)	0.929 (1)	0.779 (2)	0.785 (2)
75	0.704 (5)	0.706 (5)	0.617 (5)	0.620 (5)	0.522 (6)	0.524 (4)

(−23.96 %), while as $F_2^{(1)}/M/F_2^{(3)}$ comparing with the metal-rich shell, those increase slightly from (+17.53 %) to (+18.43 %) and from (+22.3″%) to (+22.62 %), respectively.

When the magnitudes of critical axial load for U-SSF is compared to other STs, the effect of F_1 and F_2-type coatings on dimensionless axial loads is greater at around 0.4 % and 1 % at small values ofa/h. Although the effects of TSSs on the critical axial load (or frequency parameter) for all cylindrical shells for Par- and Cos-Hyp-SSFs are approximately the same, some differences arise when U-SSF is used. For example, the effects of TSSs on the dimensionless critical axial loads of M/C/M,$F_1^{(1)}/C/F_1^{(3)}$, C/C/C and C/M/C,$F_2^{(1)}/M/F_2^{(3)}$, M/M/M shells in the parabolic or cosine hyperbolic case are 9.33 %, 6.34 %, 8.7 % and 9.04 % 14.21 %, 9.79 %, respectively, whena/h = 20, while those effects decrease and are found to be 0.33 %, 0.29 %, 0.38 % and 0.28 %, 0.49 %, 0.58 %, respectively, whena/h = 75. If the shear stress function is uniform; the effects of TSSs on the dimensionless critical axial loads of M/C/M,$F_1^{(1)}/C/F_1^{(3)}$, C/C/C and C/M/C,$F_2^{(1)}/M/F_2^{(3)}$, M/M/M cylindrical shells are 7.82 %, 5.5 %, 7.27 % and 7.54 %, 11.42 %, 8.17 %, respectively, asa/h = 20 while these effects are 0.33 %, 0.29 %, 0.38 % and 0.28 %, 0.49 %, 0.38 %, respectively, asa/h = 75. The transverse shear stress effects on the frequency parameter fora/h = 20 are approximately-two times lower than the effects on the critical axial load for Par-, Cos-Hyp- and U-SSFs. At large values of the a/h ratio, the difference between them also decreases, as the shear stress effects decrease.

In addition, while the difference between the effect of shear stresses on the critical axial load of $F_1^{(1)}/C/F_1^{(3)}$ shells for Par- and U-SSFs is 0.79 %, this difference is 2.45 % for $F_2^{(1)}/M/F_2^{(3)}$ shells, asa/h = 20, and this difference decreases and disap-

Table 5 Variation of Ω_{1ST}^{CC} and Ω_{1CT}^{CC} for clamped sandwich and monolayer cylindrical shells depending on the a/h for three different SSFs.

	$\Omega_{1ST}^{CC}(n)$	$\Omega_{1CT}^{CC}(n)$	$\Omega_{1ST}^{CC}(n)$	$\Omega_{1CT}^{CC}(n)$	$\Omega_{1ST}^{CC}(n)$	$\Omega_{1CT}^{CC}(n)$
	$M/C/M$		$F_1^{(1)}/C/F_1^{(3)}$		$C/C/C$	
a/h	$f_{i,z}^{(k)} = cosh(\bar{z}) - cosh(1/2)$ and $f_{i,z}^{(k)} = 1 - 4\bar{z}^2$ $(i = 1,2,\ k = 1,2,3)$					
20	0.789 (1)	0.825 (1)	1.041 (1)	1.073 (1)	1.378 (1)	1.437 (1)
30	0.595 (1)	0.605 (1)	0.776 (1)	0.785 (1)	1.027 (1)	1.044 (1)
50	0.450 (3)	0.452 (3)	0.582 (3)	0.584 (3)	0.765 (2)	0.768 (2)
75	0.368 (6)	0.369 (6)	0.476 (6)	0.477 (6)	0.626 (6)	0.627 (6)
a/h	$f_{i,z}^{(k)} = 1$					
20	0.794 (1)	0.825 (1)	1.045 (1)	1.073 (1)	1.387 (1)	1.437 (1)
30	0.597 (1)	0.605 (1)	0.777 (1)	0.785 (1)	1.030 (1)	1.044 (1)
50	0.450 (3)	0.452 (3)	0.582 (3)	0.584 (3)	0.766 (2)	0.768 (2)
75	0.368 (6)	0.369 (6)	0.476 (6)	0.477 (6)	0.626 (6)	0.627 (6)
	$C/M/C$		$F_2^{(1)}/M/F_2^{(3)}$		$M/M/M$	
a/h	$f_{i,z}^{(k)} = cosh(\bar{z}) - cosh(1/2)$ and $f_{i,z}^{(k)} = 1 - 4\bar{z}^2$ $(i = 1,2,\ k = 1,2,3)$					
20	0.894 (1)	0.934 (1)	0.740 (1)	0.790 (1)	0.605 (1)	0.634 (1)
30	0.661 (1)	0.672 (1)	0.554 (1)	0.569 (1)	0.451 (1)	0.459 (1)
50	0.484 (1)	0.486 (1)	0.409 (1)	0.412 (1)	0.335 (2)	0.336 (2)
75	0.396 (5)	0.397 (5)	0.336 (6)	0.337 (5)	0.274 (6)	0.275 (6)
a/h	$f_{i,z}^{(k)} = 1$					
20	0.900 (1)	0.934 (1)	0.749 (1)	0.790 (1)	0.610 (1)	0.634 (1)
30	0.662 (1)	0.672 (1)	0.557 (1)	0.569 (1)	0.452 (1)	0.459 (1)
50	0.484 (1)	0.486 (1)	0.410 (1)	0.412 (1)	0.335 (2)	0.336 (2)
75	0.396 (5)	0.397 (5)	0.336 (5)	0.337 (5)	0.274 (6)	0.275 (6)

Table 6 Variation of critical parameters of clamped sandwich and monolayer cylindrical shells depending on the h_c/h_{coat} for Par-SSF.

h_c/h_{coat}	$T_{1STcr}^{CCax} \times 10^2$	$T_{1CTcr}^{CCax} \times 10^2$	$T_{1STcr}^{CCax} \times 10^2$	$T_{1CTcr}^{CCax} \times 10^2$	$T_{1STcr}^{CCax} \times 10^2$	$T_{1CTcr}^{CCax} \times 10^2$
	$M/C/M$		$F_1^{(1)}/C/F_1^{(3)}$		$C/C/C$	
2	2.594	2.852	3.034	3.240	3.590	3.921
4	2.798	3.071	3.206	3.411		
6	2.942	3.227	3.305	3.516		
8	3.045	3.336	3.367	3.586		
h_c/h_{coat}	$C/M/C$				$M/M/M$	
			$F_2^{(1)}/M/F_2^{(3)}$			
2	3.385	3.708	2.816	3.239	2.391	2.638
4	3.178	3.489	2.609	3.083		
6	3.033	3.333	2.453	2.990		
8	2.931	3.223	2.309	2.929		
h_c/h_{coat}	Ω_{1ST}^{CC}	Ω_{1CT}^{CC}	Ω_{1ST}^{CC}	Ω_{1CT}^{CC}	Ω_{1ST}^{CC}	Ω_{1CT}^{CC}
	$M/C/M$				$C/C/C$	
			$F_1^{(1)}/C/F_1^{(3)}$			
2	0.951	0.997	1.257	1.299	1.668	1.743
4	1.093	1.145	1.369	1.412		
6	1.190	1.246	1.435	1.480		
8	1.259	1.318	1.477	1.525		
h_c/h_{coat}	$C/M/C$				$M/M/M$	
			$F_2^{(1)}/M/F_2^{(3)}$			
2	1.086	1.137	0.897	0.962	0.733	0.770
4	0.968	1.014	0.827	0.899		
6	0.911	0.955	0.786	0.868		
8	0.877	0.919	0.754	0.849		

Table 7 Variation of critical parameters of $F_1^{(1)}/C/F_1^{(3)}$ and $F_2^{(1)}/M/F_2^{(3)}$ clamped cylindrical shells depending on the volme fraction index d for Par-SSF.

Volume fraction index d	$F_1^{(1)}/C/F_1^{(3)}$		$F_2^{(1)}/M/F_2^{(3)}$	
	$T_{1STcr}^{CCax} \times 10^2$	$T_{1CTcr}^{CCax} \times 10^2$	$T_{1STcr}^{CCax} \times 10^2$	$T_{1CTcr}^{CCax} \times 10^2$
0.5	3.188	3.432	2.695	3.036
1	3.034	3.240	2.816	3.239
2	2.916	3.077	2.757	3.428
d	Ω_{1ST}^{CC}	Ω_{1CT}^{CC}	Ω_{1ST}^{CC}	Ω_{1CT}^{CC}
0.5	1.384	1.436	0.847	0.899
1	1.257	1.299	0.897	0.962
2	1.148	1.180	0.918	1.024

pears as a/h increases. For frequency parameter, these differences decrease by about half as a percentage. As can be seen, the F_1-type coatings weakens the effect of shear stresses on the critical parameters in $F_1^{(1)}/C/F_1^{(3)}$-type shells, while the F_2-type coatings makes that effect more evident in the $F_2^{(1)}/M/F_2^{(3)}$-type shells. Therefore, transverse shear stresses lose their effectiveness when$a/h \geqslant 75$.

The variations of the magnitudes of$\mathrm{T}_{1STcr}^{CCax}$,$\mathrm{T}_{1CTcr}^{CCax}$, Ω_{1ST}^{CC} and Ω_{1CT}^{CC} for M/C/M,$F_1^{(1)}/C/F_1^{(3)}$, C/M/C, $F_2^{(1)}/M/F_2^{(3)}$-type sandwich, ceramic-rich and metal-rich monolayer cylindrical shells depending on the h_c/h_{coat} are presented in Table 6 for Par-SSF. The following data are used:$a/h = 25$,$l/a = 0.4$, $d = 1$, (m,n) $= (1,1)$. The magnitudes of$\mathrm{T}_{1STcr}^{CCax}$,$\mathrm{T}_{1CTcr}^{CCax}$, Ω_{1CT}^{CC} and Ω_{1ST}^{CC} increase in sandwich shells with the ceramic-rich core and decrease in sandwich shells with the metal-rich core, depending on the increase of the h_c/h_{coat} ratio. As the h_c/h_{coat} ratio increases from 2 to 8, the effects of F_1-type coatings on the dimensionless critical axial load and dimensionless frequency parameter decrease from (+16.96 %) to (+10.58 %) and from (+32.18 %) to (+17.32 %), respectively, while the effect of F_2-type coatings on the dimensionless critical axial load increases from (−16.81 %) to (−21.22 %), but that effect on the dimensionless frequency parameter decreases from (−17.4 %) to (−14.03 %), since the $F_1^{(1)}/C/F_1^{(3)}$ and $F_2^{(1)}/M/F_2^{(3)}$-type sandwich shells are compared to the M/C/M and C/M/C-type sandwich shells, respectively. In addition, the influences of coatings on the critical parameters for $F_1^{(1)}/C/F_1^{(3)}$ and $F_2^{(1)}/M/F_2^{(3)}$ -type sandwich shells are more pronounced in the Par-SSF than in the framework of CT. Similarly, as the h_c/h_{coat} ratio increases from 2 to 8, the FG coverage effects on the dimensionless critical axial load decrease from (−15.49 %) to (−6.21 %) and from (+17.78 %) to (−3.43 %), while those effects on the dimensionless frequency parameter decrease from (−24.64 %) to (−11.45 %) and from (+22.37 %) to (+2.87 %), respectively, when comparing $F_1^{(1)}/C/F_1^{(3)}$ and $F_2^{(1)}/M/F_2^{(3)}$ -type sandwich shells with ceramic-rich and metal-rich shaped single-layer shells, respectively. While the effects of TSSs on the critical parameters for M/C/M, C/M/C and $F_1^{(1)}/C/F_1^{(3)}$ type-sandwich cylindrical shells decrease weakly, when h_c/h_{coat} increases, the said effect is more pronounced than the others in the $F_2^{(1)}/M/F_2^{(3)}$-type sandwich shell, and also increases significantly. E.g; the TSSs effects on the critical axial load and frequency parameter for the $F_2^{(1)}/M/F_2^{(3)}$ sandwich shell increase from 15.02 % to 26.85 % and from 7.25 % to 12.6 %, respectively, when the h_c/h_{coat} ratio increases from 2 to 8.

The variation of$\mathrm{T}_{1STcr}^{CCax}$,$\mathrm{T}_{1CTcr}^{CCax}$, Ω_{1CT}^{CC} and Ω_{1ST}^{CC} of clamped $F_1^{(1)}/C/F_1^{(3)}$ and $F_2^{(1)}/M/F_2^{(3)}$ cylindrical shells depending on the volme fraction index d at Par-SSF are tabulated in Table 7. The following data is used to create the Table 7:$a/h = 25$,$l/a = 0.5$, $h_{core}/h_{coat} = 4$, (m,n) $= (1,1)$. The values ofT_{1STcr}^{CCax}, T_{1CTcr}^{CCax} Ω_{1ST}^{CC} and Ω_{1ST}^{CC} decrease in $F_1^{(k)}(k = 1,3)$ coated sandwich shells due to the increase of the volume fraction index,d. The values of Ω_{1ST}^{CC} and Ω_{1ST}^{CC} decrease in $F_2^{(k)}(k = 1,3)$-type coated sandwich shells, while T_{1STcr}^{CCax} and T_{1CTcr}^{CCax} first increase and then decrease due to the increase of the volume fraction index,d. The influences of coatings on the dimensionless critical parameters for $F_1^{(1)}/C/F_1^{(3)}$ and $F_2^{(1)}/M/F_2^{(3)}$ sandwich shells, respectively, show a significant increase depending on the increase of the$d$. Consideration of TSSs more significantly reduces the effect of FG coatings on the critical parameters for $F_2^{(1)}/M/F_2^{(3)}$ shells. With the increase of$d$, the influence of TSSs on the critical axial load and frequency parameter of $F_1^{(1)}/C/F_1^{(3)}$ cylindrical shells decreases, while that effect increases significantly in $F_2^{(1)}/M/F_2^{(3)}$-shaped shells. For example, at$d$ = 0.5, the effects of TSSs on the dimensionless critical axial load of $F_1^{(1)}/C/F_1^{(3)}$ and $F_2^{(1)}/M/F_2^{(3)}$-shaped shells are 7.65 % and 12.65 %, respectively, while those are 5.52 % and 24.34 %, respectively, when$d$ = 2. Similarly, at$d$ = 0.5, the effects of TSSs on the dimensionless frequency parameter of $F_1^{(1)}/C/F_1^{(3)}$ and $F_2^{(1)}/M/F_2^{(3)}$-shaped shells are 3.76 % and 6.14 %, respectively, while those effects are 2.79 % and 11.55 %, respectively, when$d$ = 2. As can be seen, the effect of TSSs on the critical load is more pronounced than the effect on the frequency parameter.

7. Conclusions

In this study, a new approach to the analytical solution of the vibration and stability problem of clamped SCSs covered by FG coatings under an axial compressive load in the framework of STs is presented. After modeling the micro and macro mechanical properties of FG-coated SCSs with various configurations, the constitutive relations and basic equations are derived using modified Donnell type theory. The governing equations of SCSs covered by FG coating are solved using

novel approximation functions satisfying the clamped boundary conditions. After confirming the accuracy of the obtained results, the influences of shear stresses, different coating profiles and volume fractions on the critical parameters are investigated in detail.

The numerical calculations and interpratations revealed the clarity of the influence of FG coatings on the values of the critical axial load and frequency for various characteristics of sandwich cylindrical shells with clamped edges and the need to take into account the results in the design. It also shows that analyzes made for structural elements with traditional coatings will not be valid for structural members coated by new generation heterogeneous composites and that all calculations need to be renewed. The current results can be applied in various fields of modern engineering applications such as nuclear, aerospace, aviation and automotive.

8. Author agreement

We confirm that, this is an original paper, has not been submitted elsewhere for publication and has not been published elsewhere.

Funding

This article has no funding support

CRediT authorship contribution statement

A.H. Sofiyev: Conceptualization, Methodology, Formal analysis, Writing – original draft. **N. Fantuzzi:** Conceptualization, Writing – review & editing.

Declaration of Competing Interest

The authors declare that they have no known competing financial interests or personal relationships that could have appeared to influence the work reported in this paper.

Appendix A. B_{ij} and C_{ij} are defined as

$$
\begin{aligned}
&C_1=\Lambda_1^1B_1+\Lambda_2^1B_2,\ C_2=\Lambda_1^1b_{12}+\Lambda_2^1B_2,\\
&C_3=\Lambda_1^1B_3+\Lambda_2^1B_4+\Lambda_1^2,\\
&C_4=\Lambda_1^1B_4+\Lambda_2^1B_3+\Lambda_2^2,C_5=\Lambda_6^1B_5,\\
&C_6=\Lambda_6^1B_6+2\Lambda_6^2,\ C_7=\Lambda_1^1B_7+\Lambda_2^1B_9+\Lambda_7^1,\\
&C_8=\Lambda_1^1B_8+\Lambda_2^1B_{10}+\Lambda_8^1,\ C_9=\Lambda_2^1B_7+\Lambda_1^1B_9+\Lambda_9^1,\\
&C_{10}=\Lambda_2^1B_8+\Lambda_1^1B_{10}+\Lambda_{10}^1,\\
&C_{11}=\Lambda_{11}^1-\Lambda_{66}^1B_{11},\ C_{12}=\Lambda_{12}^1-\Lambda_6^1B_{12},\ B_1=\tfrac{\Lambda_1^0}{\Delta},\\
&B_2=-\tfrac{\Lambda_2^0}{\Delta},\ B_3=\tfrac{\Lambda_2^0\Lambda_2^1-\Lambda_1^1\Lambda_1^0}{\Delta},\\
&B_4=\tfrac{\Lambda_2^0\Lambda_1^1-\Lambda_2^1\Lambda_1^0}{\Delta},\ B_5=\tfrac{1}{\Lambda_6^0},\ B_6=-\tfrac{2\Lambda_6^1}{\Lambda_6^0},\ B_7=\tfrac{\Lambda_9^0\Lambda_2^0-\Lambda_{15}^0\Lambda_1^0}{\Delta},\\
&B_8=\tfrac{\Lambda_{10}^0\Lambda_2^0-\Lambda_8^0\Lambda_1^0}{\Delta},\\
&B_9=\tfrac{\Lambda_7\Lambda_2^0-\Lambda_9^0\Lambda_1^0}{\Delta},B_{10}=\tfrac{\Lambda_7^0\Lambda_2^0-\Lambda_{10}^0\Lambda_1^0}{\Delta},\ B_{11}=\tfrac{\Lambda_{11}^0}{\Lambda_6^0},\\
&B_{12}=\tfrac{\Lambda_{12}^0}{\Lambda_6^0},\ \Delta=\left(\Lambda_1^0\right)^2-\left(\Lambda_2^0\right)^2
\end{aligned}
\tag{A1}
$$

in which

$$
\begin{aligned}
\Lambda_1^{k_1}&=\int_{-h/2}^{-h_2}Q_{11}^{(1)}z^{k_1}dz+Q_{11}^{(2)}\int_{-h_2}^{h_3}z^{k_1}dz+\int_{h_3}^{h/2}Q_{11}^{(3)}z^{k_1}dz,\\
\Lambda_2^{k_1}&=\int_{-h/2}^{-h_2}Q_{12}^{(1)}z^{k_1}dz+Q_{12}^{(2)}\int_{-h_2}^{h_3}z^{k_1}dz+\int_{h_3}^{h/2}Q_{12}^{(3)}z^{k_1}dz\\
\Lambda_6^{k_1}&=\int_{-h/2}^{-h_2}Q_{66}^{(1)}z^{k_1}dz+Q_{66}^{(2)}\int_{-h_2}^{h_3}z^{k_1}dz\\
&\quad+\int_{h_3}^{h/2}Q_{66}^{(3)}z^{k_1}dz,\quad k_1=1,2\\
\Lambda_7^{k_2}&=\int_{-h/2}^{-h_2}z^{k_2}I_1^{(1)}Q_{11}^{(1)}(\bar{z})\mathrm{d}z+Q_{11}^{(2)}\int_{-h_2}^{h_3}z^{k_2}I_1^{(2)}dz\\
&\quad+\int_{h_3}^{h/2}z^{k_2}I_1^{(3)}Q_{11}^{(3)}(\bar{z})dz,\\
\Lambda_8^{k_2}&=\int_{-h/2}^{-h_2}z^{k_2}I_2^{(1)}Q_{12}^{(1)}(\bar{z})\mathrm{d}z+Q_{12}^{(2)}\int_{-h_2}^{h_3}z^{k_2}I_2^{(2)}dz\\
&\quad+\int_{h_3}^{h/2}z^{k_2}I_2^{(3)}Q_{12}^{(3)}(\bar{z})dz,\\
\Lambda_9^{k_2}&=\int_{-h/2}^{-h_2}z^{k_2}I_1^{(1)}Q_{12}^{(1)}(\bar{z})\mathrm{d}z+Q_{12}^{(2)}\int_{-h_2}^{h_3}z^{k_2}I_1^{(2)}dz\\
&\quad+\int_{h_3}^{h/2}z^{k_2}I_1^{(3)}Q_{12}^{(3)}(\bar{z})dz,\\
\Lambda_{10}^{k_2}&=\int_{-h/2}^{-h_2}z^{k_2}I_2^{(1)}Q_{11}^{(1)}(\bar{z})\mathrm{d}z+Q_{11}^{(2)}\int_{-h_2}^{h_3}z^{k_2}I_2^{(2)}dz\\
&\quad+\int_{h_3}^{h/2}z^{k_2}I_2^{(3)}Q_{11}^{(3)}(\bar{z})dz,\\
\Lambda_{11}^{k_2}&=\int_{-h/2}^{-h_2}z^{k_2}I_1^{(1)}Q_{66}(\bar{z})\mathrm{d}z+Q_{66}^{(2)}\int_{-h_2}^{h_3}z^{k_2}I_1^{(2)}dz\\
&\quad+\int_{h_3}^{h/2}z^{k_2}I_1^{(3)}Q_{66}^{(3)}(\bar{z})dz,\\
\Lambda_{12}^{k_2}&=\int_{-h/2}^{-h_2}z^{k_2}I_2^{(1)}Q_{66}(\bar{z})\mathrm{d}z+Q_{66}^{(2)}\int_{-h_2}^{h_3}z^{k_2}I_2^{(2)}dz\\
&\quad+\int_{h_3}^{h/2}z^{k_2}I_2^{(3)}Q_{66}^{(3)}(\bar{z})dz,k_2=0,\ 1
\end{aligned}
\tag{A2}
$$

References

[1] A.P. Batakis, J.W. Vogan, Rocket thrust chamber thermal barrier coatings, NASA Contract Report, 1750222, 1985.
[2] D. Zenkert, The Handbook of Sandwich Construction, Engineering Materials Advisory Service Ltd, London, 1997.
[3] V. Birman, G.J. Simitses, Elliptical and circular cylindrical sandwich shells with different facings, J. Sandwich Struct. Mater. 2 (2) (2000) 152–176.
[4] T. Hirai, M. Sasaki, Vapor-deposited functionally gradient materials, JSME Int. J. 34 (1991) 123–129.
[5] M. Koizumi, FGM activities in Japan, Compos. B Eng. 28 (1-2) (1997) 1–4.
[6] B. Kieback, A. Neubrand, H. Riedel, Processing techniques for functionally graded materials, Mater. Sci. Eng., A 362 (1-2) (2003) 81–106.
[7] U. Schulz, M. Peters, F.-W. Bach, G. Tegeder, Graded coatings for thermal, wear and corrosion barriers, Mater. Sci. Eng., A 362 (1-2) (2003) 61–80.
[8] I.M. El-Galy, B.I. Saleh, M.H. Ahmed, Functionally graded materials classifications and development trends from industrial point of view, SN Appl. Sci. 1 (11) (2019) 1378.
[9] Z. Wang, K. Maruyama, F. Narita, A novel manufacturing method and structural design of functionally graded piezoelectric composites for energy-harvesting, Mater. Des. 214 (2022) 110371, https://doi.org/10.1016/j.matdes.2021.110371.
[10] D.T. Sarathchandra, S.K. Subbu, N. Venkaiah, Functionally graded materials and processing techniques: Materials Today-Proceedings 2018; 5(10):21328-21334.
[11] W. Zhang, X. Shao, W. Zhang, J. Qi, H. Li, Unknown input observer-based appointed-time funnel control for quadrotors, Aerosp. Sci. Technol. 126 (2022) 107351, https://doi.org/10.1016/j.ast.2022.107351.
[12] X.L. Shao, J.T. Zhang, W.D. Zhang, Distributed cooperative surrounding control for mobile robots with uncertainties and aperiodic sampling, IEEE Transactions on intelligent transportation systems, 10.1109 /TITS.2022.3189201.(in press).

[13] A.M. Zenkour, A comprehensive analysis of functionally graded sandwich plates: Part 2 - buckling and free vibration, Int. J. Solids Struct. 42 (18-19) (2005) 5243–5258.
[14] A.M. Zenkour, M. Sobhy, Thermal buckling of various types of FGM sandwich plates, Compos. Struct. 93 (1) (2010) 93–102.
[15] A.H. Sofiyev, Vibration and stability of composite cylindrical shells containing a FG layer subjected to various loads, Struct. Eng. Mech. 27 (3) (2007) 365–391.
[16] H.-S. Shen, S.-R. Li, Post buckling of sandwich plates with FGM face sheets and temperature-dependent properties, Compos. B Eng. 39 (2) (2008) 332–344.
[17] M. Sobhy, Buckling and free vibration of exponentially graded sandwich plates resting on elastic foundations under various boundary conditions, Compos. Struct. 99 (2013) 76–87.
[18] A.H. Sofiyev, The vibration and buckling of sandwich cylindrical shells covered by different coatings subjected to the hydrostatic pressure, Compos. Struct. 117 (2014) 124–134.
[19] M. Sobhy, An accurate shear deformation theory for vibration and buckling of FGM sandwich plates in hygrothermal environment, Int. J. Mech. Sci. 110 (2016) 62–77.
[20] F. Tornabene, S. Brischetto, N. Fantuzzi, M. Bacciocchi, Boundary conditions in 2D numerical and 3D exact models for cylindrical bending analysis of functionally graded structures, Shock VibrationVolume 2016 (2016) 1–17.
[21] F. Tornabene, N. Fantuzzi, M. Bacciocchi, E. Viola, J. Reddy, A numerical investigation on the natural frequencies of FGM sandwich shells with variable thickness by the local generalized differential quadrature method, Appl. Sci. 7 (2) (2017) 131, https://doi.org/10.3390/app7020131.
[22] A. Melaibari, R.M. Abo-bakr, S.A. Mohamed, M.A. Eltaher, Static stability of higher order functionally graded beam under variable axial load, Alexandria Eng. J. 59 (3) (2020) 1661–1675.
[23] H.B. Khaniki, S.h. Hosseini-Hashemi, A. Nezamabadi, Buckling analysis of nonuniform nonlocal strain gradient beams using generalized differential quadrature method, Alexandria Eng. J. 57 (3) (2018) 1361–1368.
[24] Q.-H. Pham, T. Thanh Tran, V. Ke Tran, P.-C. Nguyen, T. Nguyen-Thoi, Free vibration of functionally graded porous non-uniform thickness annular-nanoplates resting on elastic foundation using ES-MITC3 element, Alexandria Eng. J. 61 (3) (2022) 1788–1802.
[25] M. Shariyat, S.H. Hosseini, Novel rule-based global-local theory and energy model for sandwich plates with compliant cores and unevenly-distributed anisotropic SMA wires under impulsive/impact loads, Compos. Struct. 209 (2019) 727–738.
[26] B.o. Liu, T. Shi, Y. Xing, Three-dimensional free vibration analyses of functionally graded laminated shells under thermal environment by a hierarchical quadrature element method, Compos. Struct. 252 (2020) 112733, https://doi.org/10.1016/j.compstruct.2020.112733.
[27] A.A. Daikh, Thermal buckling analysis of functionally graded sandwich cylindrical shells, Adv. Aircraft Spacecraft Sci. 7 (4) (2020) 335–351.
[28] T. Fu, X. Wu, Z. Xiao, Z. Chen, J. Li, Vibro-acoustic characteristics of eccentrically stiffened functionally graded material sandwich cylindrical shell under external mean fluid, Appl. Math. Model. 91 (2021) 214–231.
[29] A. Garg, M.-O. Belarbi, H.D. Chalak, A. Chakrabarti, A review of the analysis of sandwich FGM structures, Compos. Struct. 258 (2021) 113427, https://doi.org/10.1016/j.compstruct.2020.113427.
[30] A. Karakoti, S. Pandey, V.R. Kar, Dynamic responses analysis of P and S-FGM sandwich cylindrical shell panels using a new layerwise method, Struct. Eng. Mech. 80 (4) (2021) 417–432.
[31] B.M. Shinde, A.S. Sayyad, A new higher order shear and normal deformation theory for FGM sandwich shells, Compos. Struct. 280 (2022) 114865, https://doi.org/10.1016/j.compstruct.2021.114865.
[32] M. Ramezani, M. Rezaiee-Pajand, F. Tornabene, Nonlinear dynamic analysis of FG/SMA/FG sandwich cylindrical shells using HSDT and semi ANS functions, Thin-Walled Struct. 171 (2022) 108702, https://doi.org/10.1016/j.tws.2021.108702.
[33] M. Avey, N. Fantuzi, A.H. Sofiyev, Thermoelastic stability of CNT patterned conical shells under thermal loading in the framework of shear deformation theory, Mech. Adv. Mater. Struct. (2022), https://doi.org/10.1080/15376494.2022. 2045653.
[34] M. Avey, N. Fantuzzi, A. Sofiyev, Mathematical modeling and analytical solution of thermoelastic stability problem of functionally graded nanocomposite cylinders within different theories, Mathematics 10 (7) (2022) 1081, https://doi.org/10.3390/math10071081.
[35] A. Houshangi, A.A. Jafari, S.E. Haghighi, M. Nezami, Supersonic flutter characteristics of truncated sandwich conical shells with MR core, Thin-Walled Struct. 173 (2022) 108888, https://doi.org/10.1016/j.tws.2022.108888.
[36] C. Li, J. Yang, H.-S. Shen, Postbuckling of pressure-loaded auxetic sandwich cylindrical shells with FG-GRC face sheets and 3D double-V meta-lattice core, Thin-Walled Struct. 177 (2022) 109440, https://doi.org/10.1016/j.tws.2022.109440.
[37] S. Rekhviashvili, A. Pskhu, P. Agarwal, S. Jain, Application of the fractional oscillator model to describe damped vibrations, Turkish J. Phys. 43 (3) (2019) 236–242.
[38] G. Rajchakit, R. Sriraman, N. Boonsatit, P. Hammachukiattikul, C.P. Lim, P. Agarwal, Global exponential stability of Clifford-valued neural networks with time-varying delays and impulsive effects, Adv. Difference Equations 208 (2021) 1–21.
[39] G. Rajchakit, R. Sriraman, N. Boonsatit, P. Hammachukiattikul, C.P. Lim, P. Agarwal, Exponential stability in the Lagrange sense for Clifford-valued recurrent neural networks with time delays, Adv. Difference Equations 256 (2021) 1–21.
[40] G. Rajchakit, P. Agarwal, S. Ramalingam (Eds.), Stability Analysis of Neural Networks, Springer Singapore, Singapore, 2021.
[41] H.-S. Shen, Postbuckling analysis of axially-loaded functionally graded cylindrical shells in thermal environments, Compos. Sci. Technol. 62 (7-8) (2002) 977–987.
[42] H.-S. Shen, Postbuckling of axially-loaded FGM hybrid cylindrical shells in thermal environments, Compos. Sci. Technol. 65 (11-12) (2005) 1675–1690.
[43] H.S. Shen, Functionally Graded Materials, Nonlinear Analysis of Plates and Shells, CRC Press, Florida, 2009.
[44] A.H. Sofiyev, On the vibration and stability of clamped FGM conical shells under external loads, J. Compos. Mater. 45 (7) (2011) 771–788.
[45] A.H. Sofiyev, A.N. Alizada, Ö. Akin, A. Valiyev, M. Avcar, S. Adiguzel, On the stability of FGM shells subjected to combined loads with different edge conditions and resting on elastic foundations, Acta Mech. 223 (1) (2012) 189–204.
[46] J.N. Reddy, Mechanics of Laminated Composite Plates and Shells: Theory and Analysis, 2nd ed., CRC Press, New-York, 2004.
[47] A.S. Volmir, The Nonlinear Dynamics of Plates and Shells, Nauka, Moscow, 1972 [in Russian].
[48] M.R. Eslami, Buckling and Postbuckling of Beams, Plates and Shells. Springer, Switzerland, 2018.
[49] C.T. Loy, K.Y. Lam, C. Shu, Analysis of cylindrical shells using generalized differential quadrature, Shock Vib. 4 (3) (1997) 193–198.
[50] X.M. Zhang, G.R. Liu, K.Y. Lam, Vibration analysis of thin cylindrical shells using wave propagation approach, J. Sound Vib. 239 (3) (2001) 397–403.
[51] K.Y. Lam, C.T. Loy, Effects of boundary conditions on frequencies of a multi-layered cylindrical shell, J. Sound Vib. 188 (3) (1995) 363–384.